International Journal of Concrete Structures and Materials
Vol.7, No.2, pp.127–133, June 2013
DOI 10.1007/s40069-012-0027-7
ISSN 1976-0485 / eISSN 2234-1315

Computer Aided Design of RC Structures

S. M. Shahidul Islam*, and A. Khennane

(Received August 5, 2012, Accepted December 31, 2012)

Abstract: After reviewing the background and motivations for using modern computational methods for the design of reinforced concrete structures, an algorithm making use of the object oriented programming language Python and professionally developed finite element software is presented for the sizing and placement of the reinforcement in RC structures. The developed method is then used to design the reinforcement of a deep beam. To validate the design, two identical deep beam specimens were manufactured with the obtained steel, and then tested in the laboratory. It was found that the experimental results corroborated those predicted with the finite element design method.

Keywords: automated design, non-linear finite element analysis, python, object oriented programming, deep beams.

1. Introduction

Since the first application of the finite element to the analysis of reinforced beams by Ngo and Scordelis (1967), a large number of approaches for modeling the behavior of concrete as a material or the behavior of reinforced concrete structures have been developed. While it is not the aim of the present study to provide a detailed review of the very large body of literature on this subject, as there are many good quality reviews published in the literature (ASCE 1982; de Borst 2002), it is still worthwhile to briefly describe some of the major developments that have occurred in this area.

Ngo and Scordelis (1967) analyzed simple beams using a triangular element. The cracking of concrete was modeled using the discrete approach. This approach, which is physically and intuitively appealing, was implemented by letting a crack grow when the nodal force at the node ahead of the crack tip exceeded a tensile strength criterion. Then, the node is split into two nodes and the tip of the crack is assumed to propagate to the next node. This process, of course, requires the redefinition of the mesh every time a crack propagates. This proved computationally intensive even in two dimensions, let alone in three dimensions. This prompted Rashid (1968) to develop the smeared crack approach, where a crack is numerically, rather than physically, modeled. In this approach, cracking of the concrete occurs when the principal tensile stress exceeds the ultimate tensile strength. The elastic modulus of the material is then assumed to be zero in the direction parallel to the principal tensile stress direction. Since these pioneering works, many other developments have taken place; in particular the experimental work of Kupfer et al. (1969), Palaniswamy and Shah (1974), and Kotsovos and Newman (1977), which revealed many aspects of the peculiar behavior of concrete such as exhibiting nonlinearity in both tension and compression, and its failure envelope depended on all the stress invariants. This prompted the development of failure criteria for concrete (Willam and Warnke 1975; Ottosen 1977), and plasticity based models (Chen 1976). Up to the middle of the 80s, the classical plasticity based models formed the majority of the constitutive models for concrete. Yet, they still could not capture the progressive degradation of the mechanical properties caused by the initiation and coalescence of micro-cracks. Notable developments in this area were the recognition that concrete is not a completely brittle material and crack orientation changes with loading history (Vecchio and Collins 1982). This led to the development of strain softening models. Hillerborg (1976) developed the fictitious crack model, which considers a tension softening fracture zone to avoid stress concentration at the tip of the crack. Recognizing that micro-cracking in the fracture process zone is not continuous, Bazant and Oh (1983) introduced the crack band model. Another significant contribution was the development of the rotating crack model (Cope et al. 1980; Gupta and Akbar 1983; de Borst and Nauta 1985; Rots 1988). The 80s have also seen the development of continuum damage mechanics as a framework for modeling degradation of the mechanical properties of concrete (Mazars 1984; Mazars and Pijaudier-Cabot 1989). When combined with plasticity, damage models; such as the ones proposed by Lubliner et al. (1989) and Lee and Fenves (1998), form a powerful class of models capable of describing the macroscopic behavior of concrete. The later have been implemented in the commercial finite element software ABAQUS (Simulia 2011).

Yet despite more than four decades of research and a large body of literature on the application of finite elements in the analysis of reinforced concrete, very few of these

School of Engineering and Information Technology,
The University of New South Wales, Canberra,
ACT, Australia.
*Corresponding Author; E-mail: smislam93@yahoo.com

achievements have reached the design office; the finite element is still used as a verification tool rather than as a design tool. Hu and Lin (2006) analysed a PWR prestressed concrete containment vessel to verify its structural integrity under internal pressure. More recently, Syroka et al. (2011) and Mercan et al. (2010) analyzed reinforced concrete corbels and prestressed spandrel beams respectively, and on both occasions the finite element predictions were compared with experimental results. There have been few attempts at using the finite element method as a design tool for reinforced concrete structures (Tabatai and Mosalam 2001; An and Maekawa 2004; Khennane 2005). Unlike in other fields of engineering; such as metal forming, where numerical simulations are being conducted on a routine basis to design industrial parts (Khelifa et al. 2007), or the automobile industry, which simulates crash tests extensively even though it is possible to develop a product solely through prototyping, automated design of concrete structures has not attracted a lot of attention. This lack of interest can be explained by the difficulties associated with modeling the complex behavior of reinforced concrete, and by the fact that civil engineering structures are unique. The other likely reason is the impossibility to assess the validity of finite element designed structures with actual proof testing because of their size.

The aim of the present study therefore is to use the finite element method to design reinforced structural elements, which can be manufactured and subsequently tested to validate the designs. A deep beam is chosen because its behavior encompasses all the difficulties associated with modeling reinforced concrete structures under a state of generalized stress, and also for the ease of manufacture and testing. The technique, initially developed by Khennane (2005), which consists in using professional software because of user friendliness and proven reliability as opposed to "in-house" written software was adapted. The general purpose finite element code ABAQUS was selected. ABAQUS not only offers robust concrete models such as the one based on the concept of damaged plasticity theory developed by Lubliner et al. (1989) and Lee and Fenves (1998)., but it also comes with a scripting interface, which is an extension of the object oriented programming language Python (2011). For instance in ABAQUS, it is possible to write a Python script that automates the following tasks: creating and modifying the components of a model, such as parts, materials, loads, and steps; creating, modifying, and submitting analysis jobs; reading from and writing to the output databases; and, viewing the results of an analysis.

2. Design Principles and Methodology

2.1 Finite Element Modelling

Before optimizing the reinforcement, it is necessary to develop a finite element model for the reinforced concrete deep beam. Two dimensional four-node continuum plane stress (CPS4) elements were used to model the concrete while two nodded truss elements were used for the reinforcement. Perfect bond was assumed between the reinforcement and the surrounding concrete. This was achieved by embedding the truss elements in the continuum elements representing the concrete. This type of representation allows the reinforcement to be treated as an integral part of the basic element, and its stiffness contribution can be evaluated using the principle of superposition.

The ABAQUS damage plasticity model (CDPM) was used to model the behaviour of the concrete. The input parameters required for defining this material model are the concrete compression hardening, compression damage, tension softening, tensile damage and dilatation angle. The compression stress–crack opening displacement curve proposed by Wee et al. (1996) shown in Fig. 1 was used to obtain the concrete compression hardening and damage data.

The tension softening and damage data are generated from the tensile stress–strain relationship proposed by Hordijk (1991) as illustrated in Fig. 2.

The dilatation angle was assumed to be 50°. A detailed description of the CDPM model and its implementation can be found in the ABAQUS 6.10 documentation (Simulia 2011). It is worth to note that the CDPM is primarily intended for the analysis of concrete under cyclic/dynamic loading. And as such, it includes material softening and stiffness degradation, which at times, can lead to convergence difficulties. These can be avoided by using a viscoplastic regularization of the constitutive equations.

A linear elastic perfectly plastic model was used for the reinforcement bars. Because of symmetry in both loading and geometry, only half the model is analysed as shown in Fig. 3. The boundary condition XSYMM ($u_x = 0$, $\phi_y = 0$ and $\phi_z = 0$) was applied to the symmetry plane and a retrained y-displacement was applied at the left support.

To validate the model and hence gain enough confidence in using it in a performance design, its predictions are compared to the experimental test results obtained by Tanimura and Sato (2005) as shown on Fig. 4. To study the mesh sensitivity, different element sizes, 25, 40, and 50 mm, were tried. The results from the coarse meshes show better agreement with the experimental results. This corroborates the findings of Malm (2006) who also noticed that in ABAQUS coarse meshes give slightly better results. As a result, the 50 mm element size is adopted for the remaining of the analyses because it is also computationally less expensive.

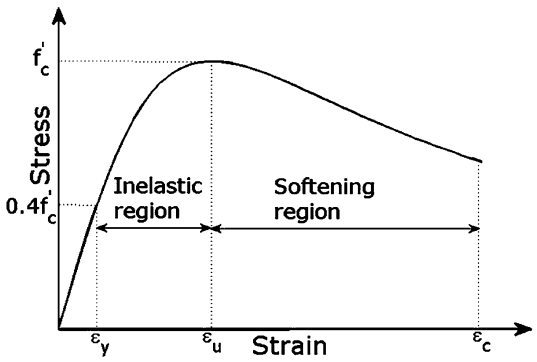

Fig. 1 Concrete compression model.

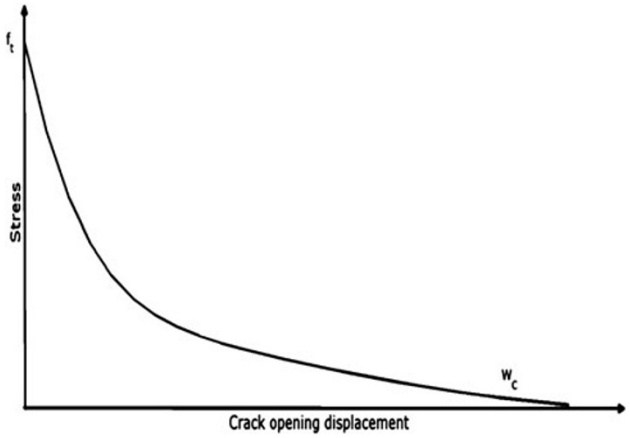

Fig. 2 Concrete tensile model.

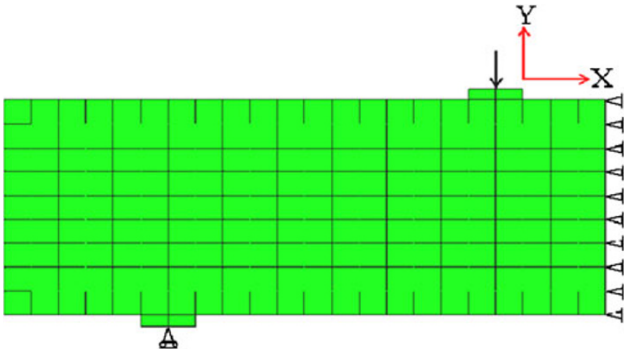

Fig. 3 Geometry and boundary conditions.

2.2 Design Methodology

The developed finite element method described and validated in above is used to design a deep beam, whose dimensions are shown in Fig. 5. The beam should be capable of supporting a total load of 450 kN. The criterion for the design is that the reinforcement should be strained as close as possible to its yielding limit without exceeding it. The yield strength of the reinforcement and the compressive strength of the concrete are chosen as 500 and 55 MPa, respectively for this design.

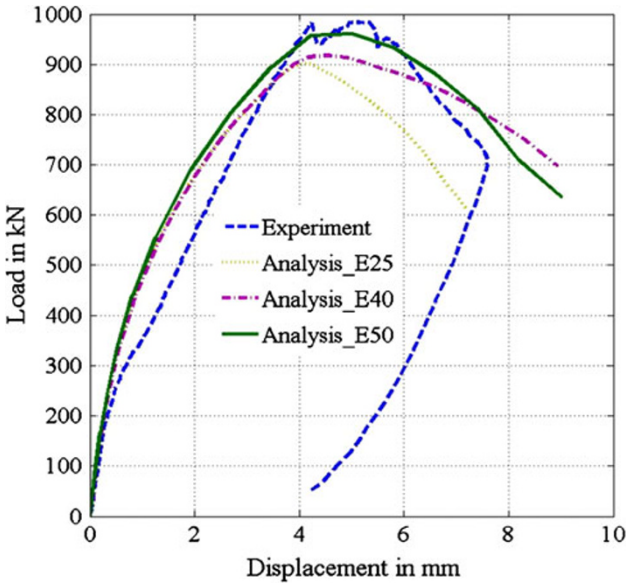

Fig. 4 Mesh sensitivity and model validation.

The methodology for the design is schematically shown in Fig. 6. Initially the beam, without any reinforcement, is analyzed as a linear elastic medium to identify the areas of potential cracking. A minimum reinforcement is then incorporated in these areas (hereafter named reinforcing fields) and the target design load is applied in increments. The analysis is carried out in a non-linear fashion, and the amount of reinforcement is updated as required. At the end of a load increment, and before the solution proceeds to the next step, the reinforcement is checked whether it has yielded or not. If no yielding has occurred, the analysis progresses to the next load increment. Otherwise, the reinforcement is updated as to avert yielding. Updating the reinforcement also heals the stiffness of the beam, and as such eliminates convergence difficulties, which results from stiffness degradation. The design process is carried out iteratively until the target load has been achieved and no yielding is detected. The steps in the algorithm are implemented using the object oriented programming language Python. This iterative process combined with a nonlinear analysis takes about 1 h on a Windows machine with Intel Core 2 Quad CPU Q6600 processor running at 2.40 GHz. However, improvements in hardware coupled to parallel processing, should make it feasible for use in practice on large scale structures.

As mentioned previously, the criterion is that the steel should be strained as close as possible to its yield strain. Of course, other criteria such a limiting deflection or a crack opening could be used separately or in conjunction with steel yielding, but that is more a case of generalization rather than one of principle. To avert yielding of the reinforcement, the smart fictitious material model for steel is used for this purpose. The steel model is reversed to decide the amount of reinforcement as shown in Fig. 7. The calculated stress σ_n, either in tension or compression, is compared to the yield stress σ_y. If the calculated stress is less than the yield stress, no action is taken. Otherwise, the new area of steel required to inhibit yielding is obtained as:

$$A = A_0 \frac{\sigma_n}{\sigma_y} \tag{1}$$

where A is the updated steel area and A_0 is the initial steel area. This process is equivalent to a plasticity algorithm where the state of stress is scaled back to the yield surface. However, instead of redistributing the excess stress as a pseudo-load vector as done in a plastic analysis, it is the area of steel that is increased to keep the strain just at yielding. A detailed description of this process termed strengthening behaviour as opposed to plastic behaviour is explained in Hoogenboom (1998).

Applying the first step in the algorithm described in Fig. 6, results in the strain contour plots of the beam analyzed as linear elastic medium (Fig. 8). It can be clearly seen that there are regions of high tensile and compressive strains respectively at the bottom and the top parts of the beam in

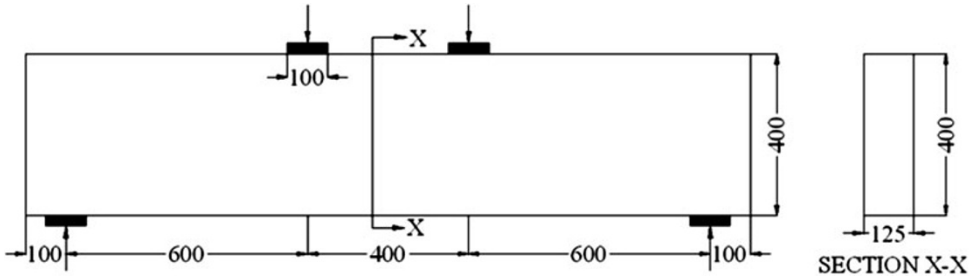

Fig. 5 Dimensions in mm and loading.

BEGIN

Step 1: Load the Abaqus Solver to read the input file and carry out a linear analysis to identify the regions of potential cracking. It is important to make sure that the job is run interactively.

Step 2: Group all the elements belonging to regions of potential cracking into element sets, called herein reinforcing fields.

Step 3: Provide these reinforcing fields with minimum reinforcement ratios.

Step 4: Set the target load for which the reinforcement is to be optimised, and divide it into load increments.

Step 5: While the applied load is less that the target load

- Carry out a nonlinear analysis of the current model
- Access the Abaqus database file (extension .odb)
- Loop through the reinforcing fields (elements sets) and retrieve the maximum and minimum strains at the reinforcement level, and check whether the reinforcement has yielded or not.

IF no yielding of reinforcement
- Load = load + load_increment

ELSE
- Update any reinforcement that has yielded.
- Keep load constant.

END IF

END

Fig. 6 Automated design process.

the flexural span. In addition, it can be observed that the direction of the principal strains changes to 45° in the shear regions. Based on these regions of high strain intensities, seven reinforcing fields are identified for the solid beam as shown in Fig. 9. They are named according to their positions, and then translated into element sets in ABAQUS, and each assigned with an initial φ10 mm bar.

As the load increases, and because of the nonlinear behavior of the concrete and the resulting stress redistribution, the steel areas do not increase uniformly in the reinforcing fields as shown in Fig. 10. The first yielding occurred in the flexural reinforcing field BF2 at an applied load of 162 kN. The next reinforcing field to yield is the flexural reinforcement in the shear spans BF1. This takes place at a load of 300 kN. The reinforcement in the compressive region TF2 starts to yield at a load of 398 kN. It can be also noticed that the target load of 450 kN is reached without any shear reinforcements (SF1, SF2 and SF3) and compressive reinforcement (TF1) yielding, thus keeping the original φ10 bars provided. When it reaches the target load of 450 kN, the reinforcement in the tensile region BF1 and BF2 have increased from 157 mm^2, (equivalent to 2 φ10) to 402.32 mm^2 (equivalent to 2 φ16) and 778.2 mm^2 (equivalent to 4 φ16) respectively. The reinforcement in the compressive region TF2 on the other hand has increased from 157 mm^2 (equivalent to 2 φ10) to 410.43 mm^2 (equivalent to 3 φ10 and 1 φ16). The reinforcement details hence obtained are shown in Fig. 11.

3. Experimental Validation

To validate the design presented in Fig. 11. Two identical beams were cast as shown in Fig. 12. Type GP Ordinary Portland cement, crushed stone and river sand were used for the concrete mix. The maximum size of coarse aggregate was 10 mm. The concrete mix ratio was 1:2.266:1.971 and the water cement ratio was 0.5. The beam specimens and the cylinders were cured for 28 days. The cylinders were tested on the same day as the beams at 28 days of age. The compressive strength was found to vary between 53 and 55 MPa. Deformed steel bars were used for the longitudinal and

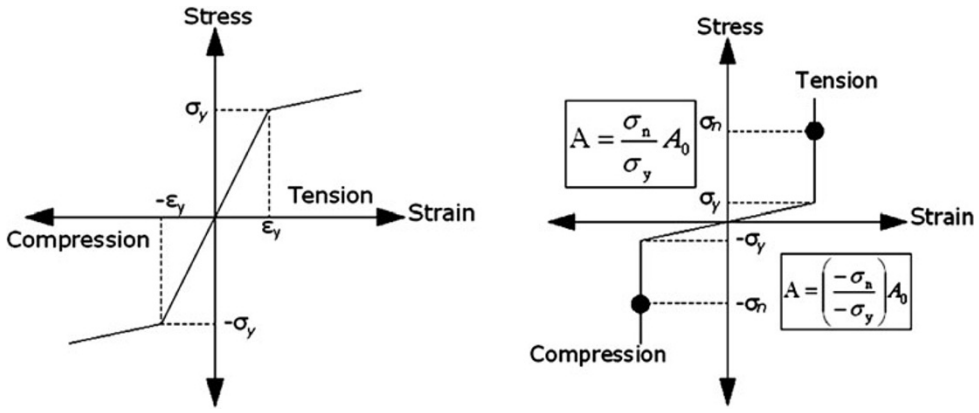

Fig. 7 Smart fictitious model.

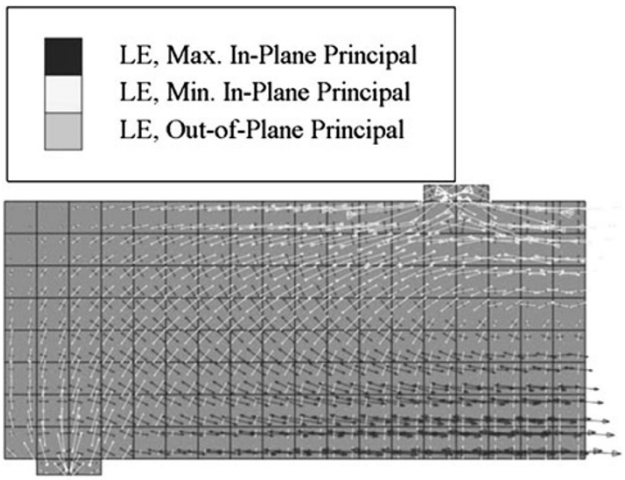

Fig. 8 Linear elastic analysis for the identification of regions of potential cracking.

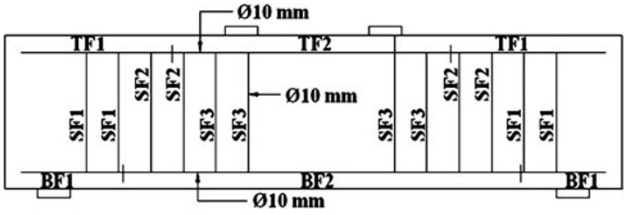

Fig. 9 Reinforcing fields.

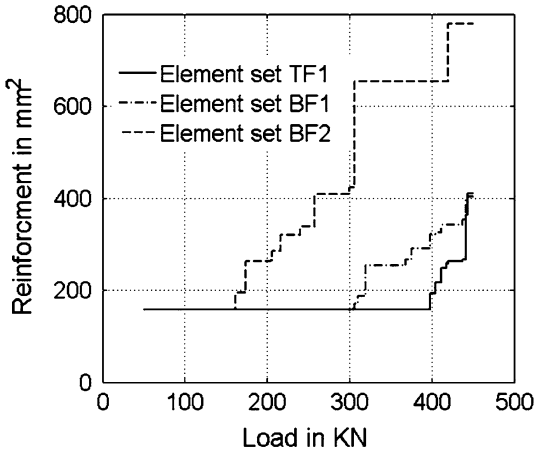

Fig. 10 Increase in steel areas.

transverse reinforcements. Their yield strength was 500 MPa.

The beams were tested under four-point bending as shown in Fig. 13. Displacement control mode was adopted at an increment 0.5 mm/min until the beams either completely failed or their resistance decreased with increasing deformation. To record the strains in the steel, strain gauges were attached to the horizontal bars at various locations.

Figure 14 shows the experimental load versus deflection curves for beams B1 and B2 as well as the computed load deflection curve. It can be seen that the failure loads of the beams B1 and B2 are different even though the beams are identical. This can only be attributed to experimental scatter. As can be observed, the tested failure loads are very close to the ultimate load carrying capacity for which the beams were designed for. Most importantly, the design resulted in a very ductile behavior as is proven experimentally.

Figure 15 shows the experimental and anticipated strain distributions in the bottom reinforcement when the applied load reaches the target load. This figure shows the strains at the locations where the strain gauges were mounted. The results show that the longitudinal steel is slightly overstrained in the flexural zone as the recorded strains exceed the yield strain for both beams. Nonetheless, it can be observed that the proposed design technique uses the reinforcing steel more efficiently since most of the recorded strains at failure are within the vicinity of the yield strain of the steel.

4. Concluding Remarks

The background and motivations for using modern computational methods for the design of reinforced concrete structures are presented. An algorithm making use of professionally developed finite element software is presented for the design of the reinforcement. It was used to design the reinforcement for a deep beam whose behavior encompasses the complexities of reinforced concrete structures, and which can be easily cast and tested in the laboratory to check the design. The rationale for the design is that the steel bars carrying the loads once the concrete is cracked should be strained as close as possible to the steel yield strain. Other criteria such a limiting deflection or a crack opening could be used separately or in conjunction with steel yielding, but that is more a case of generalization rather than one of principle.

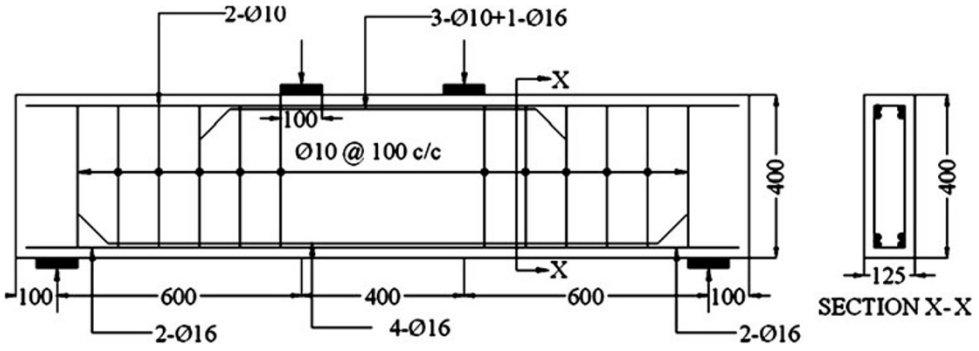

Fig. 11 FEM design (all dimensions are in mm).

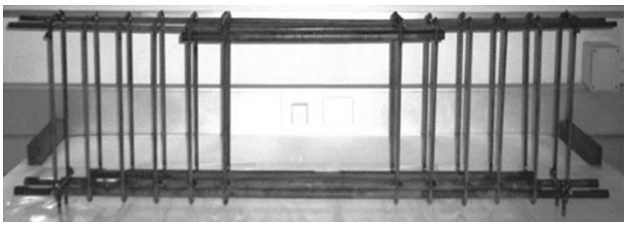

Fig. 12 Reinforcement details.

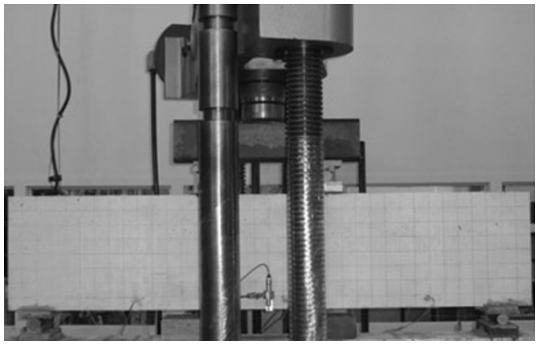

Fig. 13 Experimental setup.

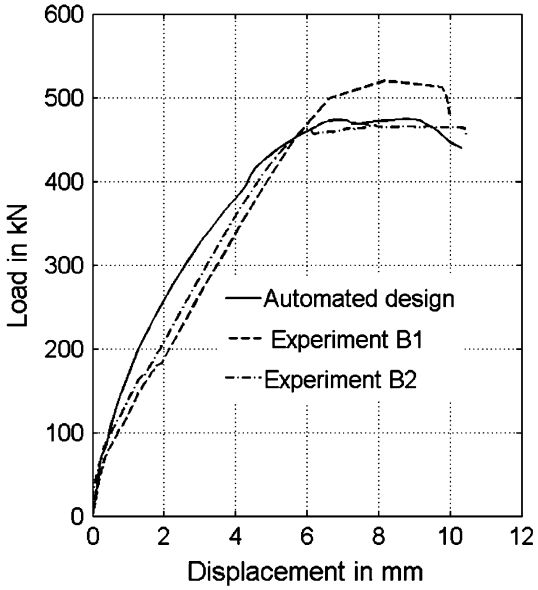

Fig. 14 Experimental load displacement curves.

To validate the design, two deep beam specimens with the obtained steel were cast and tested in the laboratory. It was found that the experimental results corroborated those predicted with the finite element design method. The failure load was found to be within 10 % of the target load. It was also found that this variation was consistent with experimental scatter. The measured mid-span displacements at failure were also consistent with those predicted by the method. It was found that the design resulted in a more ductile behavior. The measured steel strains were also found to be in the vicinity of the yield strains as anticipated by the method. Most importantly, it was experimentally proven that the method uses the reinforcing steel more efficiently.

Based on this work, it can be concluded that the current state of the art of the constitutive modeling of concrete is sufficient as to warrant the use of the finite element method

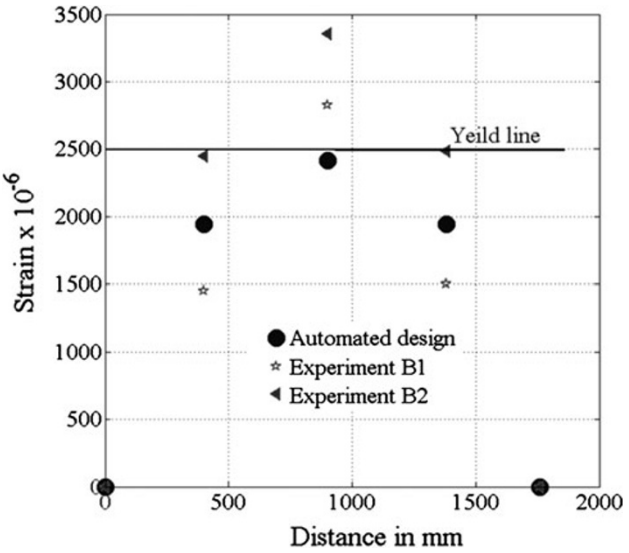

Fig. 15 Strain in tensile bars at failure.

as a design tool for reinforced concrete structures. Yet, one can still argue that the new design may not be economical after all as it involves a lot of cutting of steel bars to comply with the design. This may be true for a one-off job, but it is definitely not the case for the pre-cast industry that manufactures thousands of panels, where automated cutting and welding are used and the savings on steel could be substantial.

Open Access

References

An, X., & Maekawa, K. (2004). Computer aided reinforcement design of RC structures. *Computers and Concrete, 1*(1), 15–30.

ASCE. (1982). *Report on finite element analysis of reinforced concrete*. New York: ASCE Special Publications.

Bazant, Z., & Oh, B. (1983). Crack band theory for fracture of concrete. *Materials and Structures, RILEM, 16*, 155–176.

Chen, W. (1976). *Plasticity in reinforced concrete*. New York: McGraw-Hill.

Cope R. J., Rao P. V., Clark. L. A., & Norris. P. (1980). Modelling of reinforced concrete behaviour for finite element analysis of bridge slabs. In C. Taylor, E. Hinton, D. R. J. Owen (Eds.), *Numerical methods for non-linear problems* (pp. 457–470). Swansea, UK: Pineridge Press.

de Borst, R. (2002). Fracture in quasi-brittle materials: A review of continuum damage-based approaches. *Engineering Fracture Mechanics, 69*, 95–112.

de Borst, R., & Nauta, P. (1985). Non-orthogonal cracks in a smeared finite element model. *Engineering Computations, 2*, 35–46.

Gupta, A., & Akbar, H. (1983). A finite element for the analysis of reinforced concrete structures. *International Journal for Numerical Method in Engineering, 19*, 1705–1712.

Hillerborg, A. (1976). Analysis of crack formation and growth in concrete by means of fracture mechanics and finite element. *Cement and Concrete Research, 6*(6), 773–782.

Hoogenboom, P. C. J. (1998). *Discrete elements and nonlinearity in design of structural concrete walls*. PhD thesis, Delft University of Technology, Delft, Netherlands.

Hordijk, D. A. (1991). *Local approach to fatigue of concrete*. PhD thesis, Delft University of Technology, Delft, Netherlands.

Hu, H. T., & Lin, Y. (2006). Ultimate analysis of PWR prestressed concrete containment subjected to internal pressure. *International Journal of Pressure Vessels and Piping, 83*, 161–167.

Khelifa, M., Oudjene, M., & Khennane, A. (2007). Fracture in sheet metal forming: Effect of ductile damage evolution. *Computers & Structures, 85*(3/4), 205–212.

Khennane, A. (2005). Performance design of reinforced concrete slabs using commercial finite element software. *Structural Concrete, 6*(4), 141–147.

Kotsovos, M. D., & Newman, J. B. (1977). Behaviour of concrete under multiaxial stress. *ACI Journal, 74*(9), 443–446.

Kupfer, H. B., Hildorf, H. K., & Rusch, H. (1969). Behavior of concrete under biaxial stresses. *ACI Journal, 66*(8), 656–666.

Lee, J., & Fenves, G. L. (1998). Plastic-damage model for cyclic loading of concrete structures. *Journal of Engineering Mechanics, ASCE, 124*(8), 892–900.

Lubliner, J., Oliver, J., Oller, S., & Onate, E. (1989). A plastic-damage model for concrete. *International Journal of Solids and Structure, 25*(3), 229–326.

Malm, R. (2006). *Shear crack in concrete structures subjected to in-plane stresses.* Licentiate thesis, Department of Civil and Architectural Engineering, KTH Royal Institute of Technology, Stockholm, Sweden.

Mazars, J. (1984). *Application de la mécanique de l'endommagement au comportement non linéaire et à la rupture du béton de structure*. Thèse d'état, Université Paris VI, Paris, France (in French).

Mazars, J., & Pijaudier-Cabot, G. (1989). Continuum damage theory: Application to concrete. *Journal of Engineering Mechanics, ASCE, 115*(2), 345–365.

Mercan, B., Schultz, A. E., & Stolarski, H. K. (2010). Finite element modeling of prestressed concrete spandrel beams. *Engineering Structures, 32*, 2804–2813.

Ngo, D., & Scordelis, A. C. (1967). Finite element analysis of reinforced concrete beams. *ACI Journal, 64*(3), 152–163.

Ottosen, N. S. (1977). A failure criterion for concrete. *Journal of Engineering Mechanics, ASCE, 103*(4), 527–535.

Palaniswamy, R., & Shah, S. (1974). Fracture and stress–strain relationship of concrete under triaxial compression. *Journal of Structural Engineering, ASCE, 100*(5), 901–915.

Python Software Foundation. (2011). *Python 2.6*. Retrieved August 14, 2011, from http://www.python.org.

Rashid, Y. R. (1968). Analysis of prestressed concrete pressure vessels. *Nuclear Engineering and Design, 7*(4), 334–344.

Rots, J. G. (1988). *Computational modeling of concrete fracture*. PhD thesis, Delft University of Technology, Delft, Netherlands.

Simulia. (2011). *Abaqus documentation version 6.10*. Retrieved September 10, 2011, from http://www.simulia.com.

Syroka, E., Bobinski, J., & Tejchman, J. (2011). FE analysis of reinforced concrete corbels with enhanced continuum models. *Finite Element in Analysis and Design, 47*, 1066–1078.

Tabatai, S. M. R., & Mosalam, K. M. (2001). Computational platform for non-linear analysis/optimal design of reinforced concrete structures. *Engineering Computations, 18*(5), 726–743.

Tanimura, Y., & Sato, T. (2005). Evaluation of shear strength of deep beams with stirrups. *Quarterly Report of Railway Technical Research Institute, Japan, 46*(1), 53–56.

Vecchio, F., & Collins, M. (1982). *The response of reinforced concrete to in-plane shear and normal stress*, No. 82-03, Department of Civil Engineering, University of Toronto, Toronto, Canada.

Wee, T. H., Chin, M. S., & Mansur, M. A. (1996). Stress–strain relationship of high-strength concrete in compression. *Journal of Materials in Civil Engineering, 8*(2), 70–76.

Willam, K. J., & Warnke, E. P. (1975). Constitutive models for the triaxial behavior of concrete. *Proceedings of International Association for Bridge and Structural Engineering, 19*, 1–30.